

Clustering Eastern US Atmospheric River Types

1. Introduction

Atmospheric river (AR) is the filamentary corridor with strong horizontal poleward transport of water vapor. AR is closely related to warm conveyor belts (WCB), the ascending trajectory of extratropical cyclones, of extratropical cyclones and cold front headed low-level jet, as the definition of AR by The American Meteorological Society (AMS) Glossary of Meteorology. The amount of water an AR carry is about 7~15 Mississippi River¹. About 90% poleward transport of water vapor outside tropics is done by AR, while AR only occupy about 10% of longitude². AR doesn't just bring water vapor from tropical to mid latitude. Instead, its transportation is an evolving and transient process, with evaporation and rain out in the middle of transport process.

Over the past, integrated water volume (IWV) has been used for study characteristics of AR since it can be obtained by satellite. However, with the emergence of more reanalysis data product in recent years, integrated water vapor transport (IVT) becomes primary since it contains the information of horizontal transport by wind. IVT is the integration of moisture transport derived by multiplying specific humidity and horizontal wind from surface to 300hPa. Most of the moisture transport happens in lower atmosphere, therefore integration to 200 or 300hPa makes no significant difference.

Many AR detection and tracking methods are developed over the years. The AR detection methods can be categorized as the following types: using fixed or flexible threshold of IVT and IWV, taking the AR geometry and morphology into account, choosing a cross section, and using the intersection of the cross section and moisture field³. For the first type, if the geometry is not considered, then the moisture transport of tropical cyclone can be mis identified as AR, although tropical cyclone is round while AR is long and narrow. Therefore, the statistical result of AR identified by different

methods can vary a lot. ARTMIP is the AR tracking method intercomparison project using reanalysis data and CMIP data conducted by the AR science community. The goal of ARTMIP is to investigate uncertainties that can contribute to the difference and provide a systematic framework for tracking method comparison⁴.

Up to 30% of global precipitation and up to half of extreme precipitation⁵ is contributed by AR out of tropics. US west coast is the mostly studied places with the domineering impact of AR landfall on precipitation. However, many studies also demonstrate the significant influence of AR over central and eastern US⁶. This study would investigate different types of AR clustered by K-means, and their effect on precipitation over eastern US.

2. Data and method

The IVT data is obtained from Ramseyer's paper, with a temporal period from 1979 to 2019. Since baroclinic instability and thus intensity of storm is strongest in winter, winter time IVT data of December, January, and February is used starting from 1979 12 to 2019 2. The IVT data is calculated using 6 hourly ERA5 reanalysis data with every 25hPa from 1000 to 750hPa and every 50hPa from 750 to 300hPa, and the spatial resolution is $0.25^{\circ} \times 0.25^{\circ}$. ERA5 reanalysis data is the fifth generation of atmospheric reanalysis data of ECMWF and replaced ERA-interim. The precipitation data is from Global Precipitation Climatology Project (GPCP) version1. The temporal resolution is daily from 1996 4 to 2009, and spatial resolution is $1^{\circ} \times 1^{\circ}$. The sea surface pressure is also from ERA5.

K-means⁷⁻⁹ and Self-Organizing Maps (SOMs)⁶ are often used to cluster AR. This study implements K-means on the standardized AR IVT to cluster AR types, and set $K = 2$ after initially setting $K = 8$.

The AR identification method used is tARget version 2⁵. tARget2 is a refinement of tARget1. tARget1 is based on the 85% threshold, with a fixed lower limit of $100 \text{ kg m}^{-1}\text{s}^{-1}$.

¹, geometry requirement of length > 2000km, length/width ratio > 2, and other requirements on the coherence of IVT direction, poleward mean IVT direction, and consistency between object mean IVT direction and overall orientation³. The improvements of tARget1 are mainly using sequential threshold (85th – 95th), and filter out round objects in case they are tropical cyclones.

3. Results

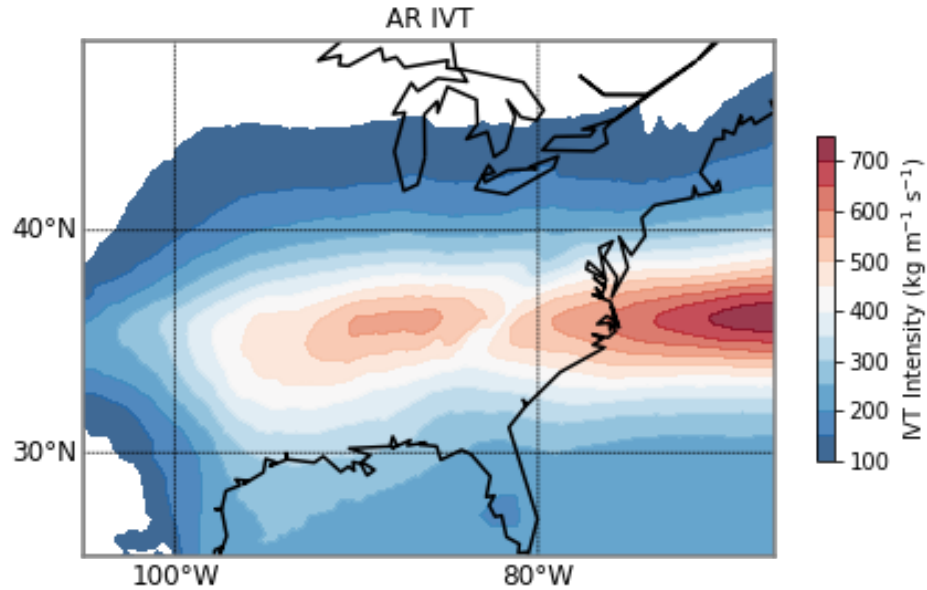


Fig 1. Composite of DJF AR IVT from 1979 12 to 2019 2.

Fig 1 is the composite of IVT of AR from 1979 12 to 2019 2. . There are two AR IVT maximum center. One is in central US with weaker, the other is on western North Atlantic with much stronger intensity.

At first, K is set to 8 considering the K-means clustering of Fish's paper and the results of clustering is shown in Fig 2. To be consistent with precipitation data, daily AR IVT is used instead of 6 hourly. AR IVT is the IVT only if AR is identified from that grid point. It is shown from the Fig 2 that the major patterns of AR IVT are two types. One with weak inland AR IVT intensity in central US and strengthened AR eastern of US continent. The other is two AR IVT maximum centers like in Fig 2. Therefore, K is changed to 2 for the following. Fig 3 is the result after applying K-means when K = 2.

The first major features of clustering when $K = 8$ corresponds to cluster 1 of Fig 3, the second one corresponds to cluster 2.

Fig 4 describes the types of precipitation. Cluster 1 is the composite of precipitation at the same time step as AR IVT cluster1, and cluster 2 is the composite of precipitation at the same time step as AR IVT cluster2. The spatial distribution of precipitation is generally reflective of distribution of AR IVT. For AR IVT cluster1, the weak inland AR intensity very likely leads to weak precipitation of cluster1 in the same region. For AR IVT cluster2, the stronger AR intensity over central US continent may cause the strong precipitation of cluster2.

If at a timestep, the AR IVT is not zero at the grid point, then the precipitation at that grid point is seen as AR precipitation. Fig 5 is the clusters of AR precipitation. The high similarity between each clusters of tells that the precipitation is mainly induced by AR activity. Cluster 2 of AR IVT displays a strong AR intensity on land, and correspondingly, the precipitation and AR precipitation of cluster 2 is heavy and penetrate further in land.

Extreme precipitation is 95% percentile of precipitation in this study. Fig6 is the clusters of AR induced extreme precipitation. AR induced extreme precipitation in cluster 2 is overall heavier than in cluster1, with an obvious maximum center northern of Mexico Gulf, suggesting the source of moisture is AR from Mexico Gulf.

Since the SLP data is only monthly, it is impossible to obtain the atmospheric circulation Pattern of each clusters. Instead, the correlation of standardized monthly mean AR IVT of each clusters and standardized SLP is obtained and shown in Fig 7.

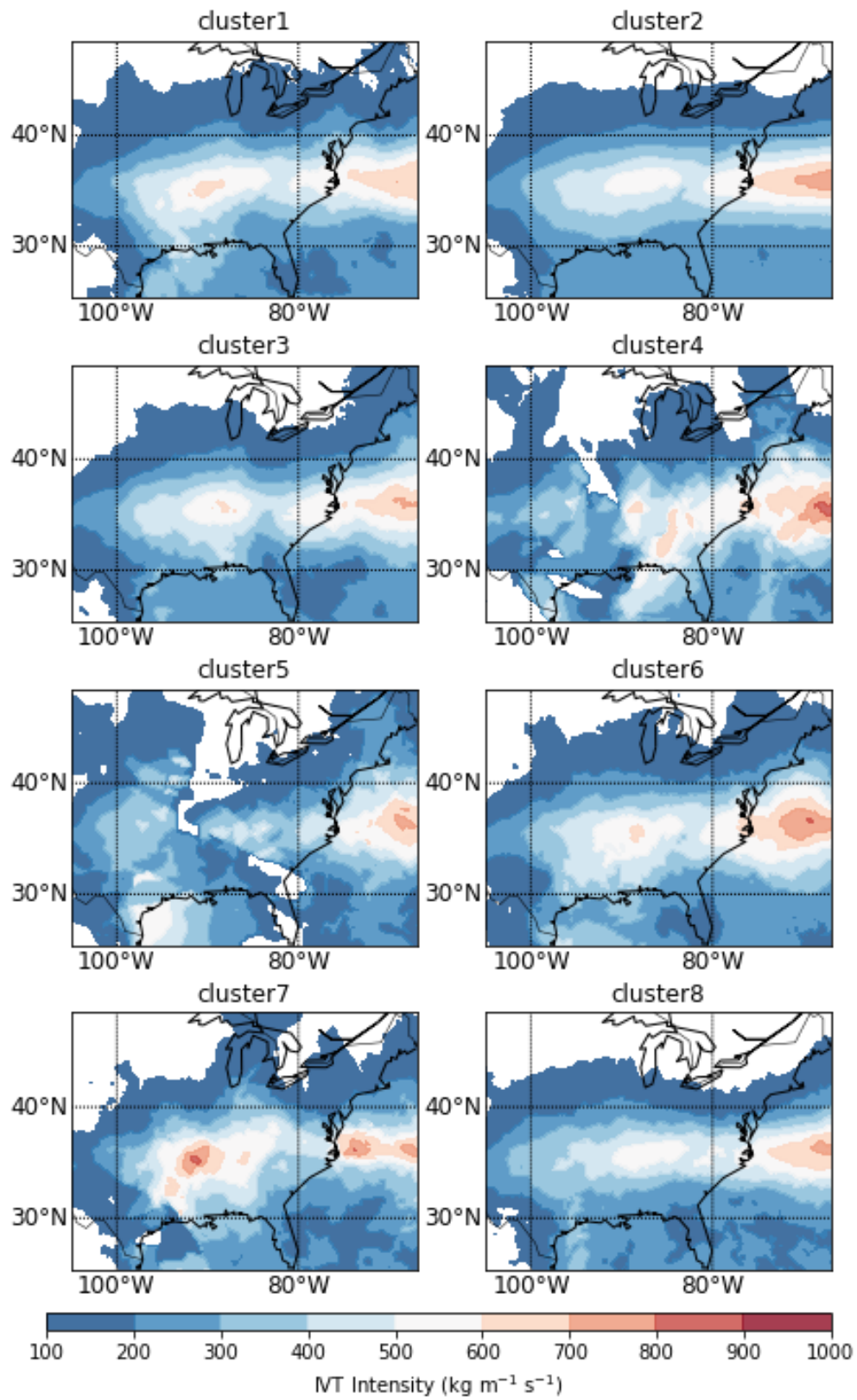


Fig 2. Cluster1 to cluster 8 of DJF AR IVT based on K-means, $K = 8$

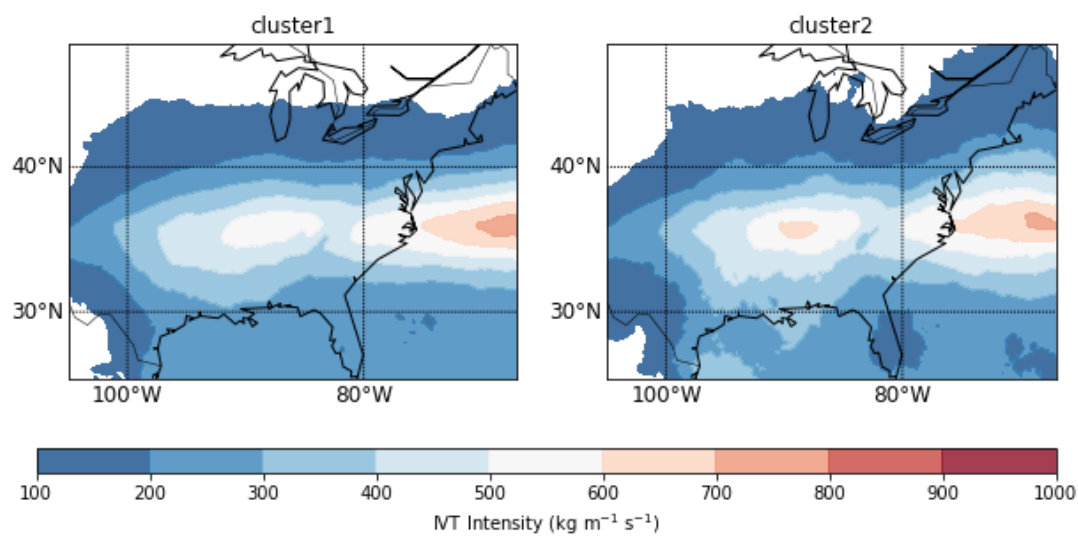


Fig 3. Clusters of DJF AR IVT when $K = 2$

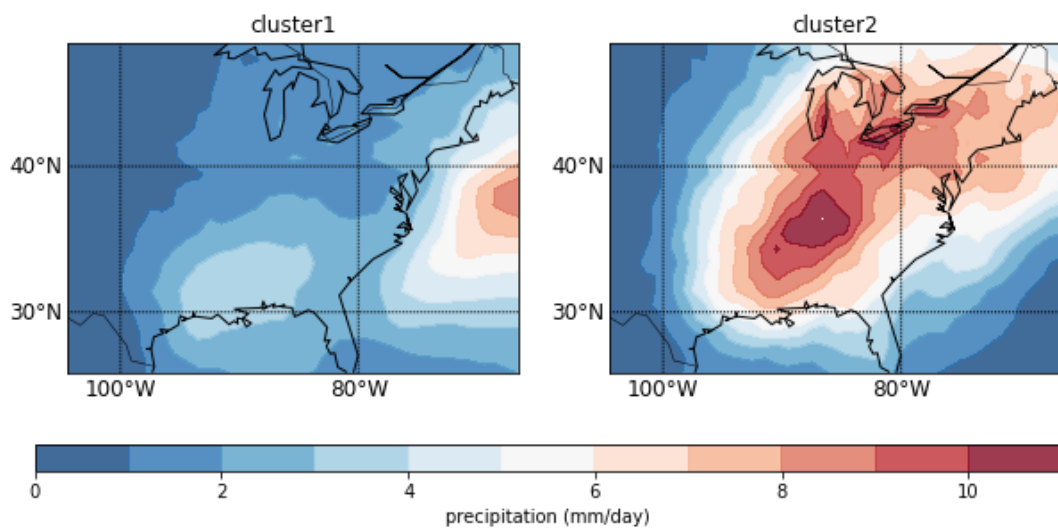


Fig 4. Clusters of DJF daily Precipitation

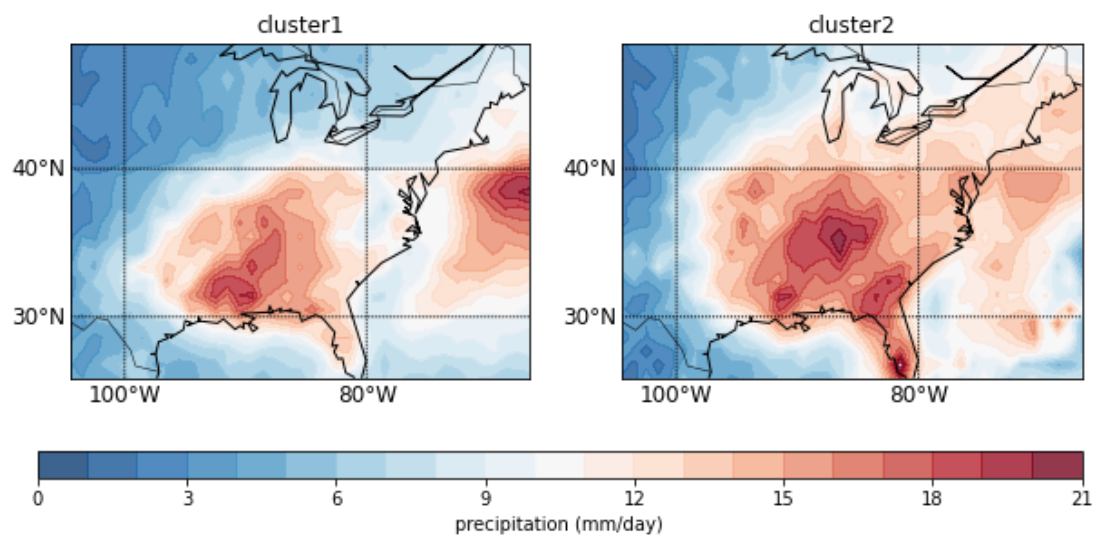


Fig 5. Clusters of DJF daily AR Precipitation

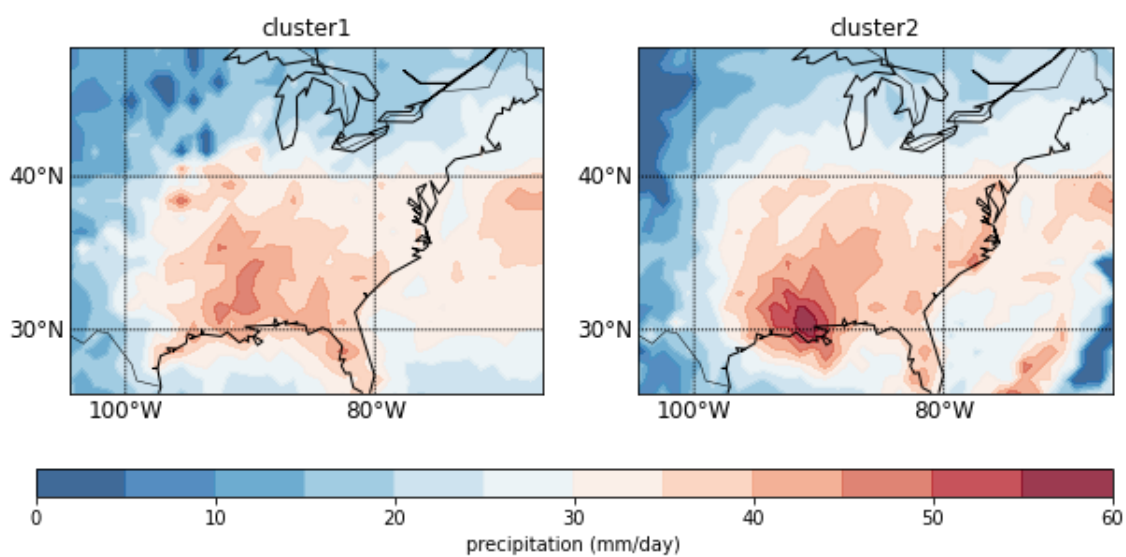


Fig 6. Clusters of DJF daily AR extreme precipitation

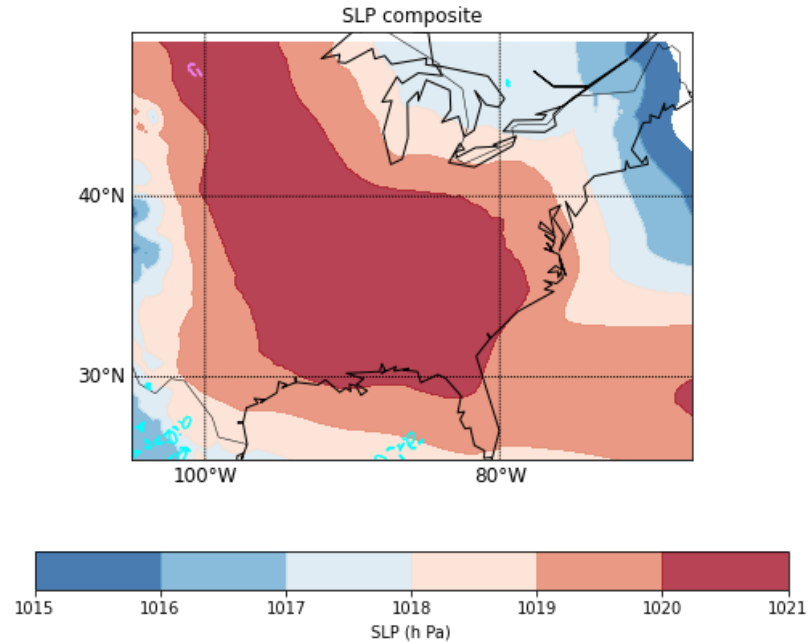


Fig 7. Composite of DJF monthly mean SLP. Cyan isolines are correlation between standardized SLP and standardized monthly mean AR IVT from cluster 1 equals 0.2 and -0.2. Violet isolines are correlation between standardized SLP and standardized monthly mean AR IVT from cluster 2 equals 0.2 and -0.2.

The correlations of both clusters are pretty small in Fig 7. From the results of Fig7, it suggests that SLP and AR IVT may not be correlated. Two ridge regression of standardized monthly mean AR IVT from cluster 1 and SLP, standardized monthly mean AR IVT from cluster 2 and SLP is conducted with regularization term selected from cross validation. However, the r^2 is too small to deem that the regression relation statistically significant. The not correlated relation of standardized monthly mean AR IVT and standardized SLP may be the reason why the regression failed.

The circulation field of west US in DJF often be characterized as a high geopotential height anomaly over west US, and a negative anomaly over eastern North Pacific, which is the Aleutian Low. The low pressure serves as trough and the high pressure center serves as ridges can steer moisture transport from North Pacific to west US. Thus, they are crucial to AR and precipitation in west US. However, the correlation result from Fig7

is basically negligible over east and central US. But this doesn't not suggest that AR at these areas is not influenced by SLP since monthly mean AR intensity is used to stay consistent with SLP data, which may not be a good representation.

4. Conclusion and Discussion

This study uses K-means to cluster two types of AR based on AR IVT. The precipitation, AR precipitation and AR extreme precipitation map from each cluster shows that AR plays a significant role in precipitation and extreme precipitation over central and eastern US. Previous study, when use K-means, chooses to base on AR duration and AR intensity. Instead of IVT, a new metric intensity duration area was designed to quantify AR intensity. The results divided AR to three types, flash AR of strong intensity and short duration, prolonged AR of strong intensity and short duration and weak AR of week intensity and short duration⁷. Fish identified types of AR families, not based on any AR characteristics or related moisture field, but based on 500hPa geopotential anomalies⁸. Six types of 500hPa anomalies are identified. However, the differences of 500hPa anomalies between clusters are mainly over North Pacific and west US. For central US, the differences are very slight and negligible. Therefore, if AR over central US impacted by SLP remains an open question. It is possible that AR intensity and AR precipitation inland is more affected by the bathymetry then SLP.

Besides SLP, the links between AR and atmospheric modes are found to be prominent. It is found out that AR is less frequent during cold phase of ENSO, and northeastern Pacific is the place where the anomalies are strongest. Over west US, La Nina induces more anticyclonic events and El Nino induces more cyclonic events. The resulting changes in ridges and troughs can cause changes of AR orientation and latitude¹⁰. Different phases of Madden-Julian oscillation (MJO) also have impact on AR on US west coast through changes in circulation, and the impact of MJO on AR is modulated by quasi-biennial oscillation (QBO)¹¹. Relations between AR and AO, PNA are also found in previous studies.

5. Reference

1. Ralph FM, Dettinger MD. Storms, floods, and the science of atmospheric rivers. *Eos, Transactions American Geophysical Union* 2011;92(32):265-266, doi:<https://doi.org/10.1029/2011EO320001>
2. Zhu Y, Newell RE. A Proposed Algorithm for Moisture Fluxes from Atmospheric Rivers. *Monthly Weather Review* 1998;126(3):725-735, doi:[https://doi.org/10.1175/1520-0493\(1998\)126<0725:APAFMF>2.0.CO;2](https://doi.org/10.1175/1520-0493(1998)126<0725:APAFMF>2.0.CO;2)
3. Guan B, Waliser DE. Detection of atmospheric rivers: Evaluation and application of an algorithm for global studies. *Journal of Geophysical Research: Atmospheres* 2015;120(24):12514-12535, doi:<https://doi.org/10.1002/2015JD024257>
4. Shields CA, Rutz JJ, Leung LY, et al. Atmospheric River Tracking Method Intercomparison Project (ARTMIP): project goals and experimental design. *Geosci Model Dev* 2018;11(6):2455-2474, doi:10.5194/gmd-11-2455-2018
5. Guan B, Waliser DE. Tracking Atmospheric Rivers Globally: Spatial Distributions and Temporal Evolution of Life Cycle Characteristics. *Journal of Geophysical Research: Atmospheres* 2019;124(23):12523-12552, doi:<https://doi.org/10.1029/2019JD031205>
6. Ramseyer CA, Stanfield TJ, Van Tol Z, et al. Identifying Eastern US Atmospheric River Types and Evaluating Historical Trends. *Journal of Geophysical Research: Atmospheres* 2022;127(17):e2021JD036198, doi:<https://doi.org/10.1029/2021JD036198>
7. Chen X, Leung LR, Gao Y, et al. Predictability of Extreme Precipitation in Western U.S. Watersheds Based on Atmospheric River Occurrence, Intensity, and Duration. *Geophysical Research Letters* 2018;45(21):11,693-11,701, doi:<https://doi.org/10.1029/2018GL079831>
8. Fish MA, Done JM, Swain DL, et al. Large-Scale Environments of Successive Atmospheric River Events Leading to Compound Precipitation Extremes in California. *Journal of Climate* 2022;35(5):1515-1536, doi:<https://doi.org/10.1175/JCLI-D-21-0168.1>
9. Ryoo J-M, Waliser DE, Waugh DW, et al. Classification of atmospheric river events on the U.S. West Coast using a trajectory model. *Journal of Geophysical Research: Atmospheres* 2015;120(8):3007-3028, doi:<https://doi.org/10.1002/2014JD022023>
10. Guirguis K, Gershunov A, Shulgina T, et al. Atmospheric rivers impacting Northern California and their modulation by a variable climate. *Climate Dynamics* 2019;52(11):6569-6583, doi:10.1007/s00382-018-4532-5
11. Mundhenk BD, Barnes EA, Maloney ED, et al. Skillful empirical subseasonal prediction of landfalling atmospheric river activity using the Madden–Julian oscillation and quasi-biennial oscillation. *npj Climate and Atmospheric Science* 2018;1(1):20177, doi:10.1038/s41612-017-0008-2